C. R. Geoscience 343 (2011) 55–71

Contents lists available at ScienceDirect

Comptes Rendus Geoscience

www.sciencedirect.com

Stratigraphy, sedimentology

Diagenetic controlled reservoir quality of South Pars gas field, an integrated approach

Qualité du réservoir contrôlé par la diagenèse du champ de gaz de South Pars, une approche intégrée

Vahid Tavakoli *, Hossain Rahimpour-Bonab, Behrooz Esrafili-Dizaji

Department of Geology, College of Science, University of Tehran, P.O. Box 14155, 6455 Tehran, Iran

ARTICLE INFO

Article history:
Received 30 December 2009
Accepted after revision 5 October 2010
Available online 3 December 2010

Presented by Bernard Tissot

Keywords:
Diagenesis
Ternary plot
Velocity-deviation log
Dolomitisation
South Pars
Iran

ABSTRACT

The Dalan-Kangan Permo-Triassic aged carbonates were deposited in the South Pars gas field in the Persian Gulf Basin, offshore Iran. Based on the thin section studies from this field, pore spaces are classified into three groups including depositional, fabric-selective and non-fabric selective. Stable isotope studies confirm the role of diagenesis in reservoir quality development. Integration of various data show that different diagenetic processes developed in two reservoir zones in the Kangan and Dalan formations. While dolomitisation enhanced reservoir properties in the upper K2 and lower K4 units, lower part of K2 and upper part of K4 have experienced more dissolution. Integration of RQI, porosity-permeability values and pore-throat sizes resulted from mercury intrusion tests shows detailed petrophysical behavior in reservoir zones. Though both upper K2 and lower K4 are dolomitised, in upper K2 unit non-fabric selective pores are dominant and fabric destructive dolomitisation is the main cause of high reservoir quality. In comparison, lower K4 has more fabric-selective pores that have been connected by fabric retentive to selective dolomitisation.

Mots clés :
Diagenèse
Diagramme ternaire
Log de déviation de vélocité
Dolomitisation
South Pars
Iran

RÉSUMÉ

Les carbonates permo-triasiques de Dalan-Kangan se sont déposés dans le champ de gaz de South Pars, dans le Golfe persique, offshore de l'Iran. A partir d'études en lame mince dans ce champ, les espaces poraux sont classés en trois groupes : dépositionnel, sélectif de texture, non sélectif de texture. Les isotopes stables confirment le rôle de la diagenèse dans le développement de la qualité du réservoir. En intégrant des données variées, on montre que des processus diagénétiques différents se développent dans deux zones réservoir, dans les formations de Kangan et Dalan. Tandis que la dolomitisation renforce les propriétés de réservoir, dans les unités supérieure K2 et inférieure K4, la partie inférieure du K2 et la partie supérieure de K4 sont l'objet d'une plus forte dissolution. L'intégration de RQI, des valeurs de porosité-perméabilité et de la taille de l'ouverture des pores résultant de tests d'intrusion de mercure, montre le comportement pétrophysique détaillé dans les zones réservoir. Bien que les unités supérieure K2 et inférieure K4 soient toutes les deux dolomitisées, dans l'unité supérieure K2, les pores non sélectifs de texture sont dominants

* Corresponding author.
E-mail addresses: vtavakol@khayam.ut.ac.ir, vahid6105@yahoo.com (V. Tavakoli).

1631-0713/$ – see front matter
doi:10.1016/j.crte.2010.10.004

et la dolomitisation destructrice de texture est la cause principale de la haute qualité du réservoir. En comparaison, l'unité inférieure K4 a plus de pores sélectifs de texture, qui ont été connectés par une dolomitisation rétentrice à sélective de texture.

1. Introduction

Diagenetic processes can enhance, create and/or destroy porosity in carbonate rocks. In essence, several studies signify that the reservoir quality is mainly controlled by the pore-geometry, which, in turn, is mainly determined by various diagenetic processes (Baron et al., 2008; Cerepi et al., 2003; Stentoft et al., 2003; Tucker and Bathurst, 1990). Accordingly, presence or absence of diagenetic imprints along with their type and intensity, play an important role in defining the ultimate reservoir quality and characteristics. As shown by many authors (Abid and Hesse, 2007; Alvarez and Roser, 2007; Ehrenberg et al., 2008; Elias et al., 2004; Esrafili-Dizaji and Rahimpour-Bonab, 2009; Rahimpour-Bonab, 2007; Rahimpour-Bonab et al., 2009) variations in diagenetic alterations such as porosity, permeability and lithology, could produce zones with different reservoir properties and so different petrophysical behaviors. The petrophysical properties such as total and effective porosity, permeability, pore-throat size and distribution are substantially affected by diagenesis type and intensity. Thus, as emphasised by many authors (Rahimpour-Bonab, 2007), carbonates reservoirs which are prone to intense diagenetic alterations, could be compartmentalised (segmented) and represent variable petrophysical properties, even in small scales. So, a procedure for the identification and characterisation of comparable diagenetic units from a petrophysical point of view, would be useful to resolve some of the key challenges faced in the exploration and production of carbonate reservoirs. As a rule of thumb, in carbonate units by progress in the diagenetic processes and so overprints, pore types and throats evolve imparting changes in petrophysical properties.

This article describes such a procedure and discusses its implications in understanding diagenetic processes that affect reservoir quality in a carbonate reservoir. Based on the integration of geological, petrophysical and isotope data as well as wireline logs, main reservoir controls were identified. The effect of each factor has been discussed in detail. In this regard, the Permo-Triassic (Upper Dalan and Kangan) reservoir intervals of South Pars gas field in Iran have been investigated. Data from three wells in offshore Persian Gulf have been documented and discussed. This procedure is particularly useful for porosity evolution studies that, in turn, are important for hydrocarbon explorations.

2. Geological setting and stratigraphy

The South Pars gas-condensate field, and its southern extension, the North Dome, are located in the Persian Gulf (Fig. 1). It is part of the huge NNE-SSW trending Qatar-Fars Arch. Qatar Arch is located in the interior platform of the Arabian Plate and bounded by the Zagros folded belt to the north and northeast. The South Pars field is actually the northern extension of the North field, located in the Iranian territory.

The major structural features of the area are the results of two main tectonic phases: the first tectonic phase is the Amar Collision that was occurred 620–640 My ago along the north-south trending Amar weak zone in the Arabian Shield. The second tectonic phase corresponds to the Najd Rift System that had occurred 530–570 million years ago, with about 300 km width and a general northwest–southeast trend, parallel to the Zagros Mountains (Al-Husseini, 2000). These major tectonic events, especially the first one, are responsible for the formation of the Qatar/Fars High and other similar structures such as the Ghawar High. Subsequent rejuvenation of the north-south structural trends controlled the structural development of the sedimentary cover and the distribution of the hydrocarbon reservoirs in the area. The Qatar-Fars High, the same as the other northerly trends, is of Precambrian basement origin. The Khuff Formation of the Arabian Plate and its equivalents Dalan and Kangan formations of Iran are thus interpreted as reflecting a major tectono-eustatic event related to the onset of rapid thermal subsidence of the early Neo-Tethys passive margin in Arabia and Iran, and the drowning of its rift shoulders (Insalaco et al., 2006).

In the Late Permian, increased accommodation space related to stretching of the crust accompanied the formation of the Neo-Tethys Ocean along the Oman-Zagros suture. The base of the resulting megasequence consists of continental to marine sandstones and shales supplied from the west. These were followed by the deposition of extensive carbonates and anhydrites (Khuff Formation in Saudi Arabia and Oman; Dalan and Kangan formations in Iran; [Al-Aswad, 1997]) over the entire Arabian shelf in shallow marine to tidal flat environments (Konert et al., 2001). Geologic traverse through Saudi Arabia to South Pars has been shown in Fig. 2.

The studied field was discovered in 1990 by drilling well SP-01 that encountered huge gas reservoirs in the Kangan-Dalan formations. In the South Pars field, gas accumulation is mostly limited to the Permian–Triassic stratigraphical units that became prospective during the 1970s following delineation of enormous gas reserves (Bordnave, 2008). Generalized Permian–Triassic stratigraphy of the South Pars field is shown in Fig. 3. In the South Pars field, the Early Permian–Early Triassic has been divided into Faraghan (Early Permian), Dalan (Late Permian) and Kangan (Early Triassic) formations (Kashfi, 2000). The Faraghan Formation is overlain disconformably by Dalan Formation that is subdivided into K5, Median Anhydrite (Nar member), K4 and K3 from bottom to the top, respectively (Fig. 3). The Median Anhydrite rests on the K5 dolomite. The succession is followed with the K4

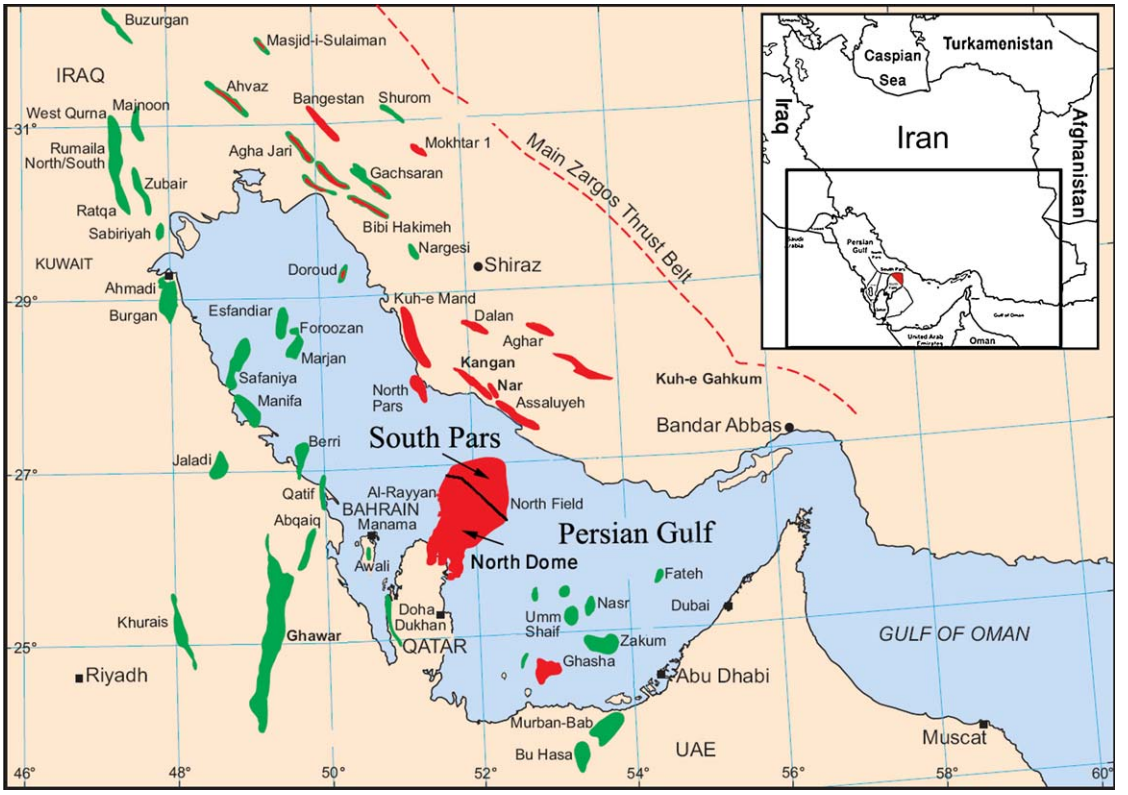

Fig. 1. Geographical and geological setting of the South Pars gas field. Main hydrocarbon fields in Persian Gulf and adjacent areas are shown. The main Zagros trust belt is clear.

Fig. 1. Site géographique et géologique du champ de gaz de South Pars. Les principaux champs d'hydrocarbures du Golfe persique et des zones adjacentes sont indiqués, ainsi que la ceinture du Zagros.

Modified from Insalaco et al. (2006).

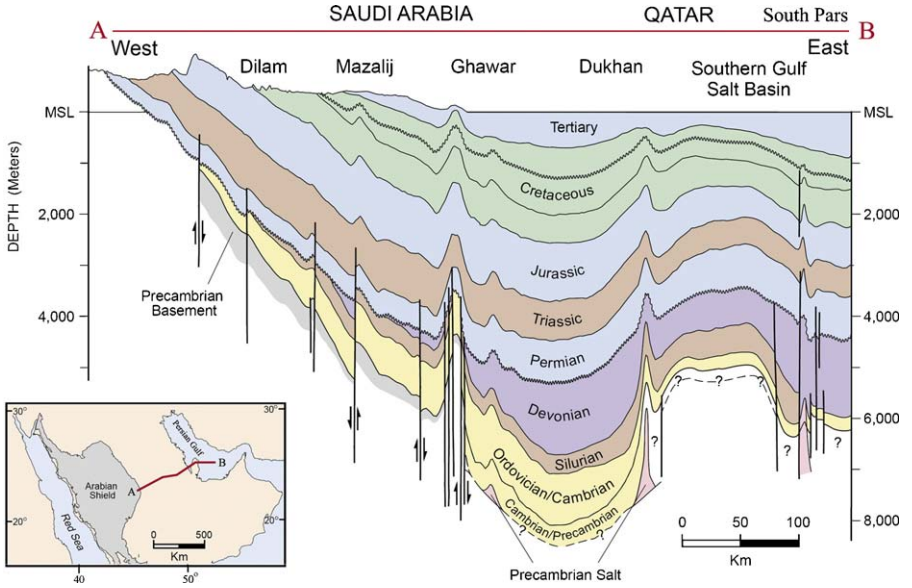

Fig. 2. Geologic traverse through Saudi Arabia to Qatar and South Pars shows the correlation between formations in these regions

Fig. 2. Une coupe géologique à travers l'Arabie saoudite jusqu'au Quatar et à South Pars montre la corrélation entre les formations de ces régions.

Modified from Konert et al. (2001).

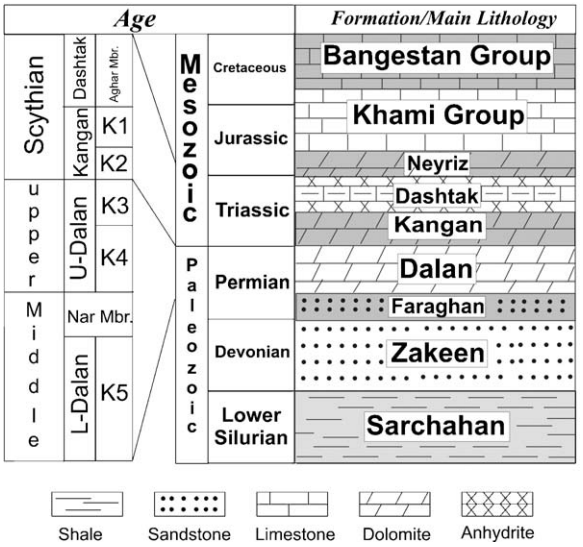

Fig. 3. Generalized stratigraphic chart of the South Pars gas field (not to scale). Formations and main lithology from Lower Silurian to Cretaceous have been shown. The age and position of Kangan and Dalan formations in stratigraphic column are mentioned. Subdivisions of these formations are clipped (for more details, see the text).

Fig. 3. Charte stratigraphique généralisée du champ de gaz de South Pars (pas à l'échelle). Les formations et la lithologie principale depuis le Silurien inférieur jusqu'au Crétacé ont été indiquées. L'âge et la position des formations Kangan et Dalan dans la colonne stratigraphique sont mentionnés. Les subdivisions de ces formations sont tronquées (pour plus de détails, voir le texte).

unit that consists of dolomite and limestone with some anhydrite intervals. The K3 member consists of dolomite with lesser amounts of dolomitic limestone. Another main reservoir unit, named Kangan in Iranian nomenclature, conformably overlies on the Late Permian strata of K3 (uppermost Dalan Formation). Szabo and Keradpir (1978) refer Kangan Formation to Early Triassic, but recent investigations by Rahimpour-Bonab et al. (2009) indicate an important gap in the Permo-Triassic boundary in this field. Limestones and dolomites of K2 and anhydritic dolomite, dolomite and limestones of K1 are constituents of this Formation. The Kangan Formation is terminated with Dashtak Formation as an efficient cap rock. Main reservoir intervals are K2 and K4 (Aali et al., 2006; Ehrenberg, 2006; Moradpour et al., 2008; Rahimpour-Bonab, 2007; Rahimpour-Bonab et al., 2009). The Field is a good representative of heterogeneous carbonate-evaporite reservoirs in the world. The lithological variations from limestone to dolomite and anhydrite control the reservoir properties that caused immense lateral and vertical changes in the porosity types and values. These, along with complicated diagenetic history, induced important heterogeneities in the reservoirs.

3. Material and methods

Our dataset consists of wireline logs, core and thin sections in about 30 cm intervals of three wells from 1200 m cores of Kangan and Dalan formations from South Pars gas fields in Persian Gulf (wells OFA_1, OFA_2 and OFA_3). Wireline logs, cores and thin sections for 12 other wells have been used for general fields study. For facies analysis, Dunham texture scheme was used together with sedimentary structures and fabrics, grain size, rock composition, and diagnostic allochems such as ooids, pelloids and shells. With careful petrographic examinations using core samples, thin sections and scanning electron microscopy (SEM), facies types, different diagenetic imprints, distribution patterns of various grains and pore types were determined. Thin sections were stained with alizarin red-S for distinguishing calcite from dolomite. Types and abundance of porosity were determined using digital point counting method. For this approach 68 thin-sectioned samples, representative of all lithofacies along the studied intervals, were examined. A total of 250 points was counted per image and between six to 10 photos prepared covering entire area of a thin section. Cleaned and dried core plug samples have been used to measure the porosity and permeability. Porosity values have been obtained by means of Boyle's law. In the routine core analysis, absolute permeabilities were obtained by gas flowing, either air or nitrogen, through the samples. Pore-throat size distributions have been achieved using mercury intrusion tests. Carbon and Oxygen isotopic data of the 348 samples from two wells were available from earlier studies (Rahimpour-Bonab et al., 2009) of the Dalan and Kangan formations. Carbon and Oxygen isotopic data from 137 limestone and dolomite samples were added in this study. Samples were powdered and then bulk powdered samples sent to the Texas A and M University's Laboratory for oxygen and carbon stable isotope analysis. For better understanding of overall distribution of porosity type, velocity deviation log (VDL) was calculated using Anselmetti and Eberli formula (Anselmetti and Eberli, 1993) and correlated with stable isotopes, core porosity and permeability, reservoir quality and diagenetic processes. All cores were studied in detail for lithofacies determination and sedimentological logs preparation.

4. Results

4.1. Depositional environment summery

In the studied formations, 14 facies types were distinguished. Theses facies and their inferred depositional model are shown in Fig. 4.

In general, five major facies belts can be recognised in the field scale: the supratidal facies association is characterised by anhydrite lithology and dolomudstones with layered, massive and nodular (chicken-wire) structures. The intertidal facies association consists of dolomudstones with fenestral and homogeneous fabrics and with algal mat boundstone and anhydrite crystals. The lagoon facies association consists of bioturbated pelloid dominated packstones to laminated mudstones. The shoal facies association is characterised by oolitic, bioclastic and intraclastic grainstones with flow structures and oolitic mudstones in back shoal setting. Finally, the offshoal facies association consists of very fine bioclastic and laminated

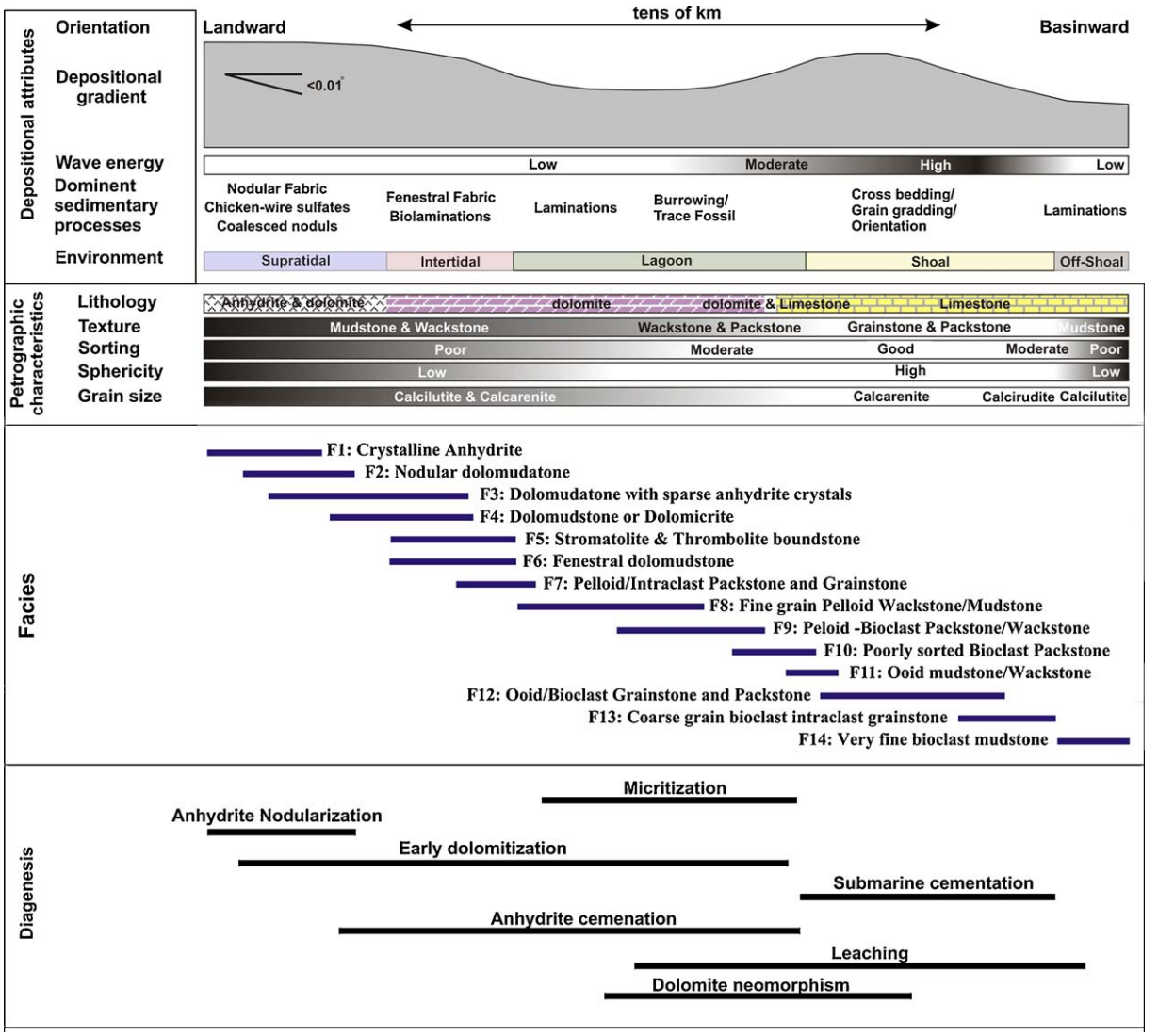

Fig. 4. Depositional environment, petrographic characteristics, facies types and distribution and diagenesis processes through the studied formations. There is not a direct relationship between these facies and reservoir quality.

Fig. 4. Milieu de dépôt, caractéristiques pétrographiques, types de faciès et leur distribution, processus diagénétiques au travers des formations étudiées. Il n'y a pas de relation directe entre ces faciès et la qualité du réservoir.

mudstones. Such depositional setting for upper Dalan-Kangan strata (upper Khuff equivalent) are also recognised and documented by other workers in outcrop sections (Zagros outcrops) and other gas fields in the Persian Gulf basin (Al-Aswad, 1997; Alsharhan and Kendall, 2003; Insalaco et al., 2006).

This depositional environment is closely comparable to the present-day Persian Gulf carbonate system, which is well-known and well documented (Alsharhan and Kendall, 2003). Seemingly, the studied strata were deposited over the inner part of such a carbonate system. Regarding to the biological evidences, inner ramp setting with a maximum water depth of 30 m is proposed here.

Petrophysical examinations of different facies types show strong variations in the porosity and permeability of the studied formations (Esrafili-Dizaji and Rahimpour-Bonab, 2009). This indicates that reservoir quality of these formations was strongly influenced by the later diagenetic processes. A comprehensive description of the upper Dalan and Kangan sedimentary environments has been shown by Esrafili-Dizaji and Rahimpour-Bonab (Esrafili-Dizaji and Rahimpour-Bonab, 2009).

4.2. Diagenesis

Based on the mineralogical compositions, cements types and occurrences, as well as main microfabrics, diagenetic environments of the studied units are distinguished and assigned to the marine, meteoric and burial realms (as observed by some authors, such as

Esrafili-Dizaji and Rahimpour-Bonab, 2009; Moradpour et al., 2008; Rahimpour-Bonab et al., 2010).

4.2.1. Marine diagenesis

Generally, the early diagenetic overprints of marine origin include micritisation, marine cementation and early stages of compaction. The petrological features of this realm include fibrous cements, skeletal micritisation, orientation of the elongated grains, early anhydrite cementation and slight deformation of grains. Marine aragonitic isopachous fringes around ooids, skeletal and non-skeletal fragments have been stabilized to calcite in the meteoric realm. These marine cements are immediately followed by clear calcite spar of phreatic or burial environment. In addition to cementation, microbial micritisation was a common process in the Kangan-upper Dalan carbonates. In the oolitic grainstones and packstones, some of the ooids and skeletal fragments show a micritic envelope, a thin and black coating around the grains. In some cases, the grain has been dissolved and the micritic envelope is still visible (Fig. S1). It is not present on all grains and its recognition can be difficult where there is isopachous cement. Circumgranular isopachous calcite cement with bladed rind is found in the oolitic grainstones either directly on the ooid or on its micritic envelope. This cement often shows dissolution either on the grain side or on the outer side.

Anhydrite cementation and nodule formation has occurred in hypersaline conditions in restricted and shallow marine environments. A comprehensive study of anhydrite formation shows that most of the anhydrites in Kangan and Dalan formations in South Pars field are primary in origin (Rahimpour-Bonab et al., 2009). This is inferred from anhydrite/dolomite relationships and cross-cutting of anhydrite with stylolites. Early dolomitization accompanied this anhydrite cements. Poikilotopic anhydrite that fills intergranular porosity is typical fabric of this diagenetic realm.

The major dolomitization phase occurred during syndepositional to shallow-burial conditions before significant burial. Petrographic evidences which support these conditions include fine crystals of dolomite that occur in early pore spaces, preservation of depositional and early diagenetic characteristics (bioturbation, micritization and marine cementation) by this type of dolomite, stylolitization and fracturing post-date dolomitization and anhydrite fabrics associated with replacive dolomites which are cut by stylolites. Most syndepositional to shallow-burial dolomites in Kangan and upper Dalan formations are fabric-retentive in texture (Fig. S1b,c). Slightly-compacted contacts between dolomitized grains suggest that this dolomitization took place before significant burial.

4.2.2. Meteoric diagenesis

The diagenesis stages continue with meteoric diagenesis during which metastable skeletal and non-skeletal grains were dissolved, generating secondary fabric- and non-fabric selective porosity. Typical freshwater cementations and dissolutions along with the polymorphic transformations of primary marine minerals all are an indication of the meteoric diagenetic realm. Petrological features typical of this realm include equant sparry calcite cement, vadose calcite silt, intragranular and intergranular dissolution pores, solution-enlarged vugs and minor gravitational cementation occurred and was recognized using optical microscopy and SEM studies. Several samples have well-developed isopachous fringes of equant calcite crystals, a few tens of μm in size (Fig. S1d). These strongly resemble cements typically formed in the shallow meteoric phreatic zone of emergent ooid shoals (e.g. Halley and Harris, 1979; James and Choquette, 1984). Some cements progressively occluded primary pore spaces. Aggrading limestone neomorphism occurred widely in various parts of the studied units (Fig. S1e).

Common textures generated in shallow meteoric diagenetic zone of Kangan and Dalan formations include fenestrae (Fig. S1f), gas-escape structures, desiccation cracks (Fig. S1g), swirling structures and planar to curviplanar grain contacts. Rocks display evidence of physical compaction but no or poorly developed stylolites, are defined to have undergone shallow-burial diagenesis.

In the studied formations, the dissolution, which usually changes and overprints other diagenetic features, could be classified into two types, i.e. freshwater (meteoric) and burial dissolution. Meteoric dissolution which is extensive and mainly fabric-selective (Figs. S1h and S2a) has occurred in the shallow meteoric realm while sediments were not completely lithified. This fabric-selective dissolution is related to the type and nature of the allochems (Fig. S2b). In wackstones and mudstones, the dissolution voids, which are isolated and irregular, show small size and partial distribution (Fig. S2c).

4.2.3. Burial diagenesis

Grading recrystallisation and chemical compaction indicate a burial diagenetic environment and its petrographic characteristics include coarse mosaic calcites with undulatory extinction, stylolites, sutured and concave-convex contacts between grains (Fig. S2d), fractures and dissolution vugs along the stylolites. Compaction, cementation and dissolution processes took place during burial of the Kangan and upper Dalan reservoir. Mechanical compaction has variably reduced porosity in oolitic grainstones and has resulted in nested fabrics (Fig. S2e). Chemical compaction, or pressure-dissolution, is an important diagenetic process in a burial environment. In addition to production of pressure-dissolution fabrics such as stylolites (Taghavi et al., 2006), the chemical compaction leads to the dissolution of grains and matrix, which is an important source of burial cements. Local and anomalous increase in horizontal permeability in some units could be related to theses stylolites (Fig. S2f).

Samples with well-developed isopachous early cements (Fig. S2g) were relatively more resistant to mechanical compaction than those without. Such samples were also less affected by pressure dissolution and contain fewer concave-convex grain contacts. Pressure dissolution also resulted in localised formation of solution seams that

concentrated non-carbonate residues (such as clays and oxide minerals). Dolomite cements are volumetrically insignificant in studied intervals. Formation of replacive dolomites led to the formation of fabric-destructive (coarse and idiotopic) dolomite bodies. Most of the fabric-destructive dolomites show stylolites "ghosts" and so they probably formed during deeper burial because they post-date stylolitization. Crystals have cloudy (inclusion-rich) cores and clear (inclusion-free) rims. Euhedral to subhedral shapes and enlarged crystal sizes result from increasing burial depths and temperatures (Fig. S2h). The same dolomite neomorphism during burial has been reported from the Khuff carbonates offshore Dubai (Videtich, 1994), and east of the Qatar Arch (Alsharhan, 2006).

Late stage anhydrite and calcite cement occluded early porosity and late fractures, which are locally important. Chicken-wire anhydrite is a product of compaction of earlier-formed anhydrite textures during burial. Burial anhydrite is also present as fracture filling cement. Late stage anhydrite forms along stylolite in some places. Fracturing and saddle dolomite cementation occurred during late phases of burial diagenesis. Theses two impacts are insignificant in overall studied units. (Ehrenberg, 2006; Guadagno and Nunziata, 1993; Kirmaci, 2008).

Burial dissolution voids usually occur in units with well-developed chemical compaction. Although the burial dissolution is not common in the study area, a few voids and solution-enlarged fractures along the stylolites could be observed.

Generalized diagenetic sequences of the studied formations along with the related porosity evolution are shown in Fig. 5, clarifying diagenetic events, environments and their relative time of formation. There is no considerable porosity-depth correlation in the field such as other fields in the Zagros Fold Belt (Ehrenberg et al., 2008).

4.3. Diagenetic imprints on the studied units

K4 Unit: This subunit, 170 m thick, consist of limestone at the top and dolomite below. Based on core analysis this unit has the highest average porosity (15.61%) with average permeability of 36.27 md. Most of the diagenetic processes in this zone are dissolution and dolomitisation. Primary pores are present especially in the upper parts. These pores have been connected in the lower parts by dolomitisation. Planar-e dolomites are most common in

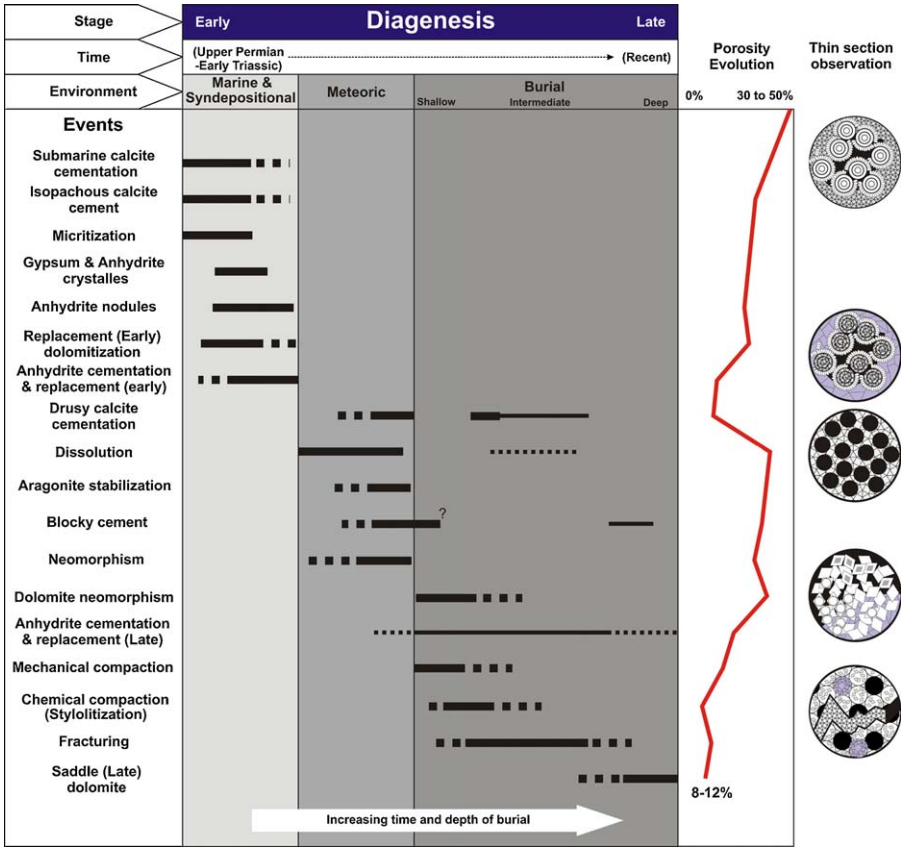

Fig. 5. Generalized diagenetic sequence of the studied formations. Time, stage and environment of various diagenetic events are clear. Porosity variation in different stages is apparent. Evidences for various diagenetic environment are mentioned.

Fig. 5. Séquence diagénétique généralisée dans les formations étudiées. La durée, l'état et l'environnement des évènements diagénétiques sont clairs. La variation de porosité au cours des différentes étapes est apparente. Les preuves d'environnements diagénétiques variés sont mentionnées.

this unit. Fabric-selective dolomitisation is dominant in domolitic intervals of this unit

Dissolution of both matrix and grains are obvious in the upper part of this unit. Fracturing has had a minor influence on porosity generation, in some cases, they have had an effect on the permeability increase. Fabric selective pores connected by fabric retentive dolomitisation are dominant porosity type in the lower part. Anhydrite is not common in K4 unit and when present, it could be seen as poikilotopic texture. As a result of increasing compaction, solution seams and stylolites are developed. These are not common in K4 unit.

K3 Unit: This unit is 133 m thick and consists of alternating limestones, dolomite and limy dolostones. Average porosity of this unit is 5.92% and average permeability is 19.21 md. This unit shows significant calcite and dolomite cementation and hence poor-to-fair reservoir quality. These cements were sometimes recrystallised. Anhydrite has been developed in various parts of the unit especially as chicken-wire texture. Calcite cement is also common. Micritisation is abundant in the Permo-Triassic boundary but could be seen in the entire unit. Ragged dark rims around the skeletal grains and irregular dark holes within them are frequently observed under the microscope and by SEM studies. They have been formed either by repeated microbial boring and subsequent micrite filling or by recrystallisation of early minerals. Some grains are fully replaced by micrite, forming black micritic casts. Bioturbation could be seen below the boundary. Compaction related phenomena such as stylolite, orientation of the elongated grains, and slight deformation of grains are present. Pervasive cementation has filled most of the pores. The remaining porosities include intercrystalline and minor fractures. Planar-s dolomites have been developed in middle part of this unit.

K2 Unit: This unit with total 44.5 m thickness consists of 15.5 m of limy dolomite and 29 m of dolomitic limestone. With average porosity of 9.71% and average permeability of 38.81 md, this unit has a good reservoir quality. The abundance of anhydrite cement (filling interparticle and oomoldic pores) decreases in this unit. Intraparticle, moldic and intercrystalline pores are the most frequent types of porosity. Intercrystalline pores are most common in the upper parts and intraparticle and moldic pores in the lower parts. Minor dissolution caused increase in the effective connection of primary pores due to lack of anhydrite cement. The presence of intercrystalline porosity as a result of dolomitisation enhanced reservoir quality by connecting the primary pores. Planar-e dolomites are most common in this unit.

As in the K4 unit, fracturing has had a minor influence on porosity generation. Permeability has been increased in rare cases when factures are open. Stylolites commonly created by chemical compaction, are not common in this unit.

K1 Unit: This unit is about 82.5 m thick and in general consists of dolomites and limy dolostones with some limestones at the middle. Average porosity is 5.78% and average permeability is 15.22 md. Anhydrite is common in this unit mainly as of blocky cements. It is a very important diagenetic event as generally caused complete pore occlusion (plugging) and drastically diminishing poroperm values. Anhydrite cementation and compaction features such as stylolite and solution seams, are the most frequent diagenetic processes observed in K1. Filled fractures were observed in some parts of the unit and fracture-filling anhydrite reduced overall poroperm values. Compaction-related effects reduced interparticle and intraparticle porosity in K1 facies. Moldic and interraparticle are the most frequent types of porosity in limestone facies, while intercrystalline porosity is mainly common in the dolomitic facies.

4.4. Ternary plot construction

Classification of carbonate pore spaces developed by Choquette and Pray (Choquette and Pray, 1970) is applicable yet, but in recent years this classification has come under criticism (Lucia, 1999, 2007). This is due to the fact that this method emphasises on the importance of pore space genesis and thus its proposed pore classes are genetic and not petrophysical (Lucia, 1999; Machel, 2005). However, consideration and modification of this classification in a new manner could provide insights into both genetical and petrophysical aspects of porosity in the carbonate reservoirs.

Because carbonate diagenesis has significant effects on the porosity creation, destruction or modification (Ahr, 2008; Machel, 2005; Moore, 2001), as well as pore types, thus identification of the pore types and their changing trends will lead to recognition of major diagenetic processes and trends. Such a method has been successfully applied to the carbonates previously (Kopaska-Merkel and Mann, 1994 for example). Ternary pore plots provide quantitative information on the shapes and origins of pore-system elements. They provide insight into a variety of geological problems, including (1) identification of flow, baffle and barrier units; i.e., stratigraphic intervals that have significantly different fluid-flow properties; (2) recognition of diagenetic processes and trends; and (3) identification and quantification of pore facies or characteristic kinds of pore systems that may be of regional extent (Kopaska-Merkel and Mann, 1994).

Here, by considering all previous studies, a new ternary plot has been introduced. In fact, by using modified genetic classification for carbonate rock porosity (Choquette and Pray, 1970), a ternary diagram whose apexes are carbonate pore types (ternary pore plots) is employed to summarize quantitative data derived from petrographical digital point counting of thin sections (Jmicrovision v1.2 Image Analysis Software) (Fig. 6). Fortunately, diagenetic changes are not difficult to identify in thin sections. Thin-section point-count data are inexpensive and easy to collect, and could be used to guide more expensive engineering analyses.

Fig. 6 shows this classification and diagenetic processes that created them. Each domain in this plot is clarified by a number that shows different degree of porosity evolution from depositional (Class 1) to completely non-fabric selective (absolutely diagenetic in origin) (Class 5). This approach simplifies the interpretation of pore systems by focusing only on three major components and by displaying these data on a simple graphic plot that makes trends

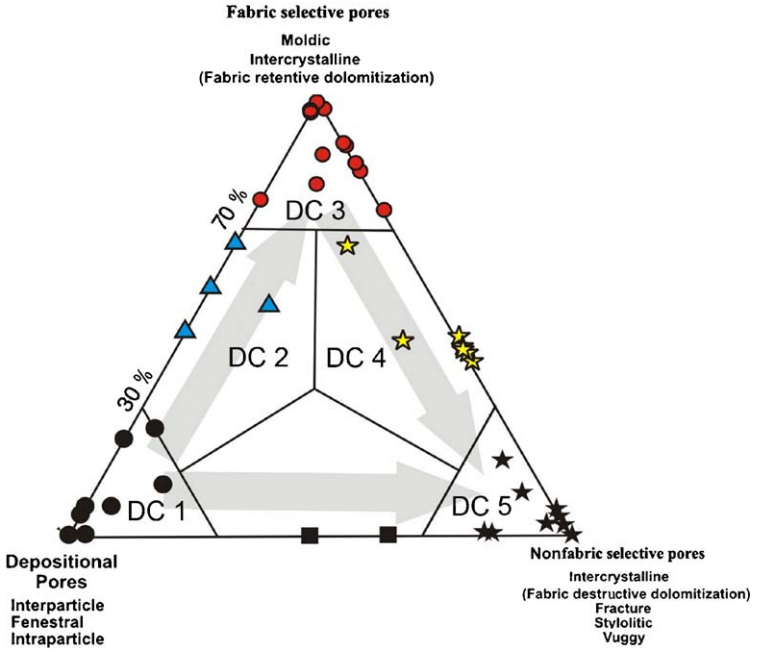

Fig. 6. Ternary plot for pore types classification. Diagenetic trends based on porosity variations are depicted. Various diagenetic processes and their impact on this trend are apparent. Depositional pores will be modified with dissolution, compaction, dolomitisation, cementation, fracturing and stylolitisation. Each of these processes make specific trend of variation in porosity type and value. Studied samples were shown with different symbols. DC is ''Diagenetic Class''.

Fig. 6. Diagramme ternaire de classification des types de pores. Les tendances diagénétiques fondées sur la porosité sont présentées. Les divers processus diagénétiques et leur impact sur la tendance mentionnée sont apparents. Les pores dépositionnels seront modifiés par dissolution, compaction, dolomitisation, cimentation, fracturation et stylolitisation. Chacun de ces processus génère une tendance spécifique de variation, dans le type et le degré de porosité. Les échantillons étudiés sont indiqués par différents symboles. DC représente la « Classe diagénétique ».

and clustering of samples clear. The utility of this technique for carbonate reservoir-rock studies has been demonstrated with examples from various parts of the world (Kopaska-Merkel and Mann, 1994 for example).

In this study, three apexes of the ternary pore plots are attributed to: (1) depositional pores (interparticle, fenestral, intraparticle); (2) fabric-selective pores (moldic and intercrystalline as well as fabric-retentive dolomitisation); and (3) non-fabric selective pores ({intercrystalline and fabric-destructive dolomitisation}, fracture, stylolite, vug) (Fig. 6). Rocks that have no primary or secondary diagenetic-mediated porosity (no visible porosity) have not any reservoir interest. These three porosity types are the most common types of pores in the Kangan and Dalan formations in South Pars gas field and account for more than 95% of total porosity in the studied thin sections. In this scheme of pore systems classification which applied to the studied carbonate reservoirs, there are five classes (Fig. 6). According to this classification scheme for the porosity, primary pores are mainly depositional (up to 70%). It means that the effect of diagenesis on the porosity formation is subordinate and intrinsic porosities are present (Class 1). Studied intervals exhibit four basic depositional pore types: (1) interparticle, (2) intraparticle, (3) shelter or keystone, and (4) fenestral pores. Shelter porosity is not common in studied Kangan and Upper Dalan intervals. So, the diagenetic Class 1 contains interparticle, intraparticle and fenestral porosities. Then diagenesis has altered primary porosities in two different ways. In the fabric-selective pore alteration scheme, porosity destruction could be due to cementation or compaction. Dissolution also could be take place after deposition. By development of fabric-selective diagenesis in this way, Class 2 is created which shows between 30 to 70% of the original depositional pores.

Progressive evolution of pores by fabric-selective diagenesis creates new porosities in the rock body which is mainly diagenetic but fabric-selective (Class 3). Class 3 typically forms in particle-supported carbonate rocks that have been partially to wholly cemented in the shallow-marine-phreatic diagenetic environment and whose particles have undergone partial to complete dissolution. The moldic pore size is determined by former particle sizes and relatively high pore/throat size (aspect) ratios. Pore size and shape are determined by the former particle boundaries; pores are commonly spherical to elliptical and several hundred micrometers across because the most common particles were peloids and ooids. Permeability values in these samples increase only slightly with increasing porosity values.

By further diagenetic alterations, the new pores mainly cross-cut primary fabrics, and thus the non-fabric selective pores (Class 4) are created. In the extreme diagenetic alterations all new pores in the rock body are completely non-fabric selective (Class 5). In the latter case, porosities could be produced due to non-fabric selective dissolution and dolomitisation, fracturing or stylolitisation. Primary rock fabric has little influence on the distribution of

intercrystalline porosity. Pore volume in the Class 5 is typically less than in the Class 3. However the aspect ratio is also smaller and a certain porosity value in this class typically corresponds to a higher permeability than in the moldic dominated strata. Although the range of porosity and mean porosity of the Class 5 is less than that of the other classes, the mean and maximum permeability is higher in the fabric-destructive intercrystalline dominated pores of this class. Fracuring could be an important factor for permeability increase in this zone. It is important to note that depositionally-mediated pore types should be distinguished from diagenetically-mediated, based on the detailed thin section studies (Fig. 6). Variations of diagenetic classes (DC) versus lithology were shown in each unit (Fig. 7).

4.5. Reservoir quality

Here, the reservoir quality prediction is addressed by identification of the main porosity and permeability controlling processes (depositional and diagenetic) and evaluating how these processes vary on the scale of interest (well, reservoir, basin). The combination of porosity and permeability data in terms of RQI (reservoir quality index), is convenient for use with the routine core analysis data that gives a tremendous advantage in addressing the reservoir quality in various scales. The concept of Amaefule et al.'s (Amaefule et al., 1993) method is based on the calculation of this term, defined as follows:

$$\mathrm{RQI} = 0.0314\sqrt{\frac{k}{\Phi}} \quad (1)$$

where: RQI: Reservoir quality index, μm; k: Permeability, md; Φ: Porosity, volume fraction.

Reservoir quality index of studied formations has been shown in Fig. 8. This value is a good representative of two basic reservoir quality indices (porosity and permeability) but size distribution of throats is not clear based on this index. Such a distribution could reveal the impact of diagenetic events on these two important factors.

Pore-throat size distributions from mercury injection capillary pressure (MICP) tests are another factor used here for evaluation of reservoir quality and impact of diagenesis. The capillary pressure curve (CPC) shows that the distribution of pore-throat sizes (PTS) are in the range 0.01–92 μm. Fig. S3 shows MICP data from eight samples through K1-K4. As it could be seen in this figure, in K1 sample (Fig. S3a) dominant pore-throat size ranges from 0.6–0.8 μm with low porosity and permeability. In upper

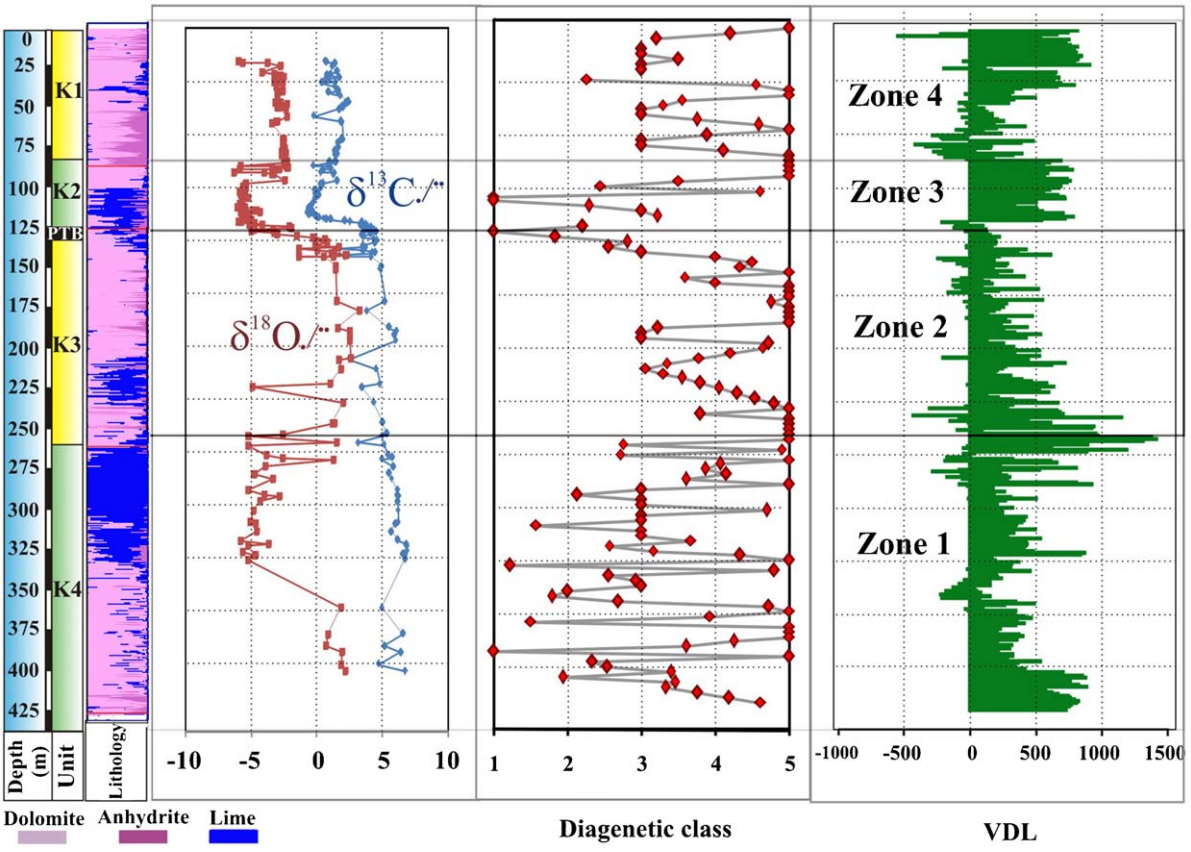

Fig. 7. Lithological percentage column, carbon and oxygen stable isotopes, diagenetic classes and velocity-deviation log for well OFA_1 illustrated beside each other. PTB boundary is seen on the units column. Four zones have been highlighted.

Fig. 7. Colonne lithologique en pourcent, avec en regard, les isotopes stables de l'oxygène et du carbone, les classes diagénétiques, le log de déviation de vélocité, pour le puits OFA_1. La limite PTB est présentée sur la colonne des unités. Quatre zones ont été mises en évidence.

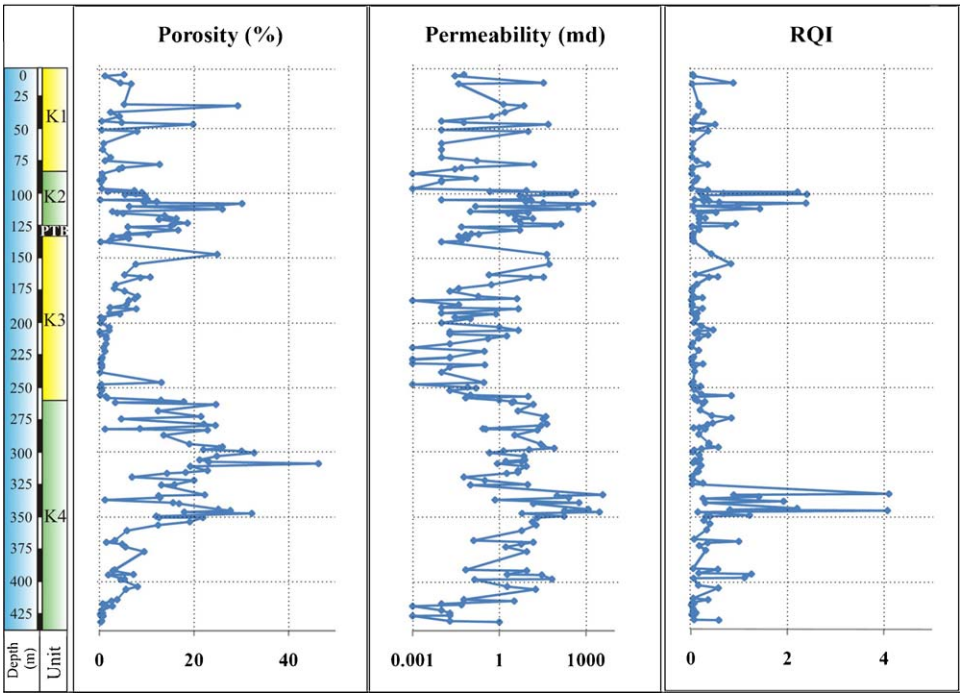

Fig. 8. Porosity, permeability and RQI of Permo-Triassic Kangan and Dalan formations in well OFA_1 of South Pars gas field derived from 430 m of cores.

Fig. 8. Porosité, perméabilité et RQI des formations permo-triasiques de Kangan et Dalan dans les puits OFA_1 du champ de gaz de South Pars, calculés à partir de 430m de carottes.

K2 sample (Fig. S3b) dolomitisation caused larger PTS with lower standard deviation. Lower K2 sample (Fig. S3c) has higher PTS dominantly range from 0.9-60 μm with higher porosity and permeability. The story of K1 unit repeats again for K3 sample (Fig. S3d) with lower mean PTS. In K3-K4 boundary with increasing rate of dissolution, dominant PTS varies toward higher values (Fig. S3e). In upper K4 unit (Fig. S3f, g) there is large PTS and high porosity and permeability. Lower K4 (Fig. S3h) has almost high permeability but porosity decreases effectively.

4.6. Oxygen and carbon isotopes

The carbon isotope data for three studied wells are illustrated in Fig. 9. Main statistical analysis of isotopic data in three wells has been shown in Table S1. $\delta^{13}C$ values show relatively constant to decreasing trends in all three wells, from base of Permian to the PTB. Close to the PTB a sudden decrease occurs from 4.14‰, 5.12‰ and 3.21‰ to −0.95‰, −0.84‰ and −0.82‰ in wells OFA_1, OFA_2 and OFA_3, respectively. Upward in the section, after this shift, a subtle increase is clear in all wells.

Wells OFA_1 and OFA_2 have a nearly complete $\delta^{18}O$ data from all over the upper Permian to lower Triassic of Kangan and upper Dalan strata. Well OFA_3 has $\delta^{18}O$ data just near the boundary (Fig. 9). These three wells show a similar trend in $\delta^{18}O$ excursions. There are higher-frequency fluctuations in K3-K4 boundary and then a subtle increase occurs from lower K3 to the top of this interval (boundary between K2 and K3). This increase is clearer in OFA_2 well. A sudden decrease occurs at Permo-Triassic boundary (PTB). In general, $\delta^{18}O$ is lower in OFA_2 well. After the PTB, $\delta^{18}O$ varies from −7.28‰ to −4.91‰ until the K1-K2 boundary in this well.

4.7. Velocity-deviation log

Combination of porosity, permeability, PTS and stable isotope data reveal quantitative reservoir properties, but pore geometry is another factor that controls reservoir quality in South Pars field. Wire-line logs are another source of information that could be used for understanding nature of pores in carbonates. The velocity-deviation log (VDL), which is calculated by combining the sonic log with the neutron-porosity or density log, provides a tool to obtain downhole information on the predominant pore type in carbonates. The log can be used to trace the downhole distribution of diagenetic processes and to estimate permeability trends (Anselmetti and Eberli, 1999) The VDL is calculated by first converting porosity-log data to a synthetic velocity log using a time-average equation (Wyllie and Gardner, 1956):

$$\frac{1}{V_{\text{rock}}} = \frac{1-\phi}{V_{\text{matrix}}} + \frac{\phi}{V_{\text{fluid}}} \tag{2}$$

The difference between the real sonic log and the synthetic sonic log can then be plotted as a velocity-deviation log. Because deviations are the result of the variability of velocity at certain porosity, the deviation log reflects the different rock-physical signatures of the different pore types.

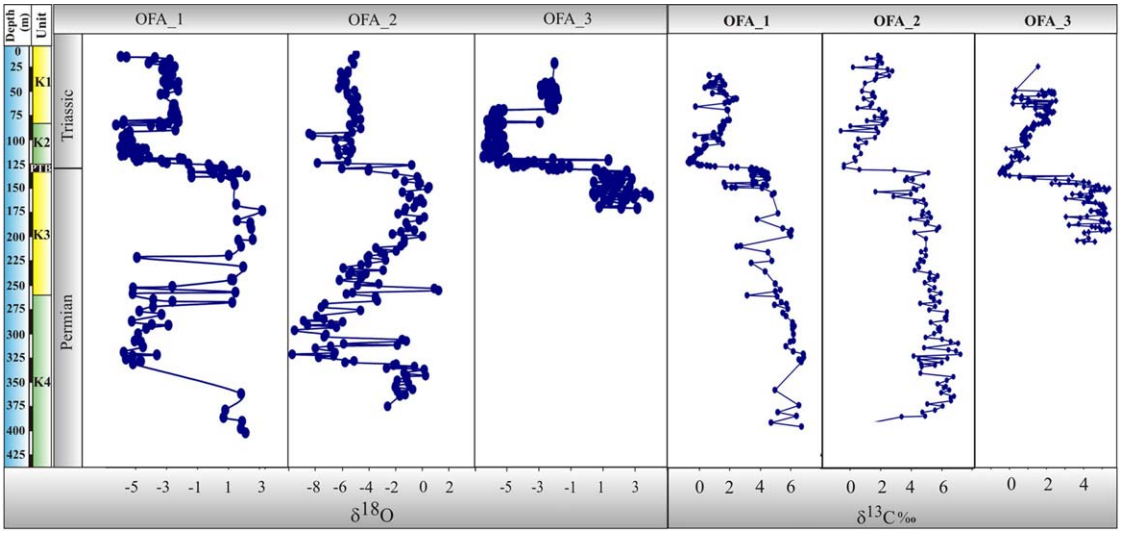

Fig. 9. Carbon and oxygen stable isotope data in three studied wells.

Fig. 9. Données sur les isotopes stables du carbone et de l'oxygène dans trois puits étudiés.

Positive deviations indicate relatively high velocities in regard to porosity, and are caused mainly by porosity that is integrated in a framelike fabric of the rock, such as in intrafossil or moldic porosity. In the moldic pores, porosity deviations indicate intense diagenetic alterations, such as dissolution or precipitation, yielding moldic porosity and favoring re-precipitation of the dissolved material as pore-filling cement.

Zones with small deviations (±500 m/s or less) represent sections that follow the predictions by the time-average equation. These zones are dominated by either interparticle, intercrystalline, or high microporosity.

There are three possible explanations for zones with the negative deviation. First this negative deviation could be the result of caving or irregularities of the borehole wall. Another reason for negative deviation is fracturing. Despite the fact that fracture porosity has always been included in the secondary porosity (equivalent to high velocity or positive deviations) (Schlumberger, 1974), several studies showed that fracturing decreases velocities on both small (Anselmetti and Eberli, 1993; Gardner et al., 1974) and large (Guadagno and Nunziata, 1993) scales. The large scale fractures can be detected with the logging tools and yield lower velocities than the undisturbed rock. In addition, buried fractures are generally closed or, in regard to total porosity, are relatively insignificant, so that the neutron porosity is not significantly reduced. As a result, fracturing produces negative deviations. These negative deviations could be also caused by a high content of free gas. Free gas would have a strong negative effect on the deviation log because gas drastically reduces Vp (Nur and Simmons, 1969) and results in a reduced neutron porosity reading due to the lower content of hydrogen in the fluid phase (Hilchie, 1982).

To produce a velocity-deviation log in the studied interval in well OFA_1, combination of neutron-porosity and porosity from density logs was used. Logs have been corrected for bad hole intervals and gas effect and then difference between real sonic and synthetic velocity was depicted.

5. Discussion

In heterogeneous carbonate reservoirs, a successful study requires integration of various data sets and methods of data analysis into a unified, interdisciplinary approach. For such an analysis, porosity and permeability data are the most critical factors. Integration of porosity and permeability data in terms of RQI provide a good relationship between these properties. Fig. 10 shows a plot of permeability versus porosity data obtained from wells OFA_2 and OFA_3. As could be seen in this figure, K1 and K3 units have no high porosity or permeability and so no reservoir quality. There are no obvious, systematic differences in porosity-permeability distribution between these units. Distinction between fabric-selective pores and non-fabric selective ones with regards to porosity-permeability characteristics can be evaluated in Fig. 10, K2 and K4 units. Upper K2 samples have higher permeability with the same porosity as lower K2 ones. Dolomitised lower K4 samples show generally higher permeability for given porosity, believed to reflect the effect of fabric destructive dolomitisation. These observations show that dolomitization enhanced permeability in both fabric-selective and fabric-destructive form. Fig. 8 shows porosity, permeability and RQI of the well OFA_1. As it is expected, porosity and permeability are higher in K4 and K2 units. RQI following porosity and permeability data has higher values in K4 and K2.

Constructing a plot of RQI versus rock texture has been shown in Fig. 11. As shown, despite wide diversity, textural categories do not occupy distinctly separate RQI fields. This shows the effect of diagenesis on the reservoir characteristics in the field. This is in agreement with the previous works on South Pars field (Esrafili-Dizaji and Rahimpour-Bonab, 2009 for example). A plot of RQI versus DCs is

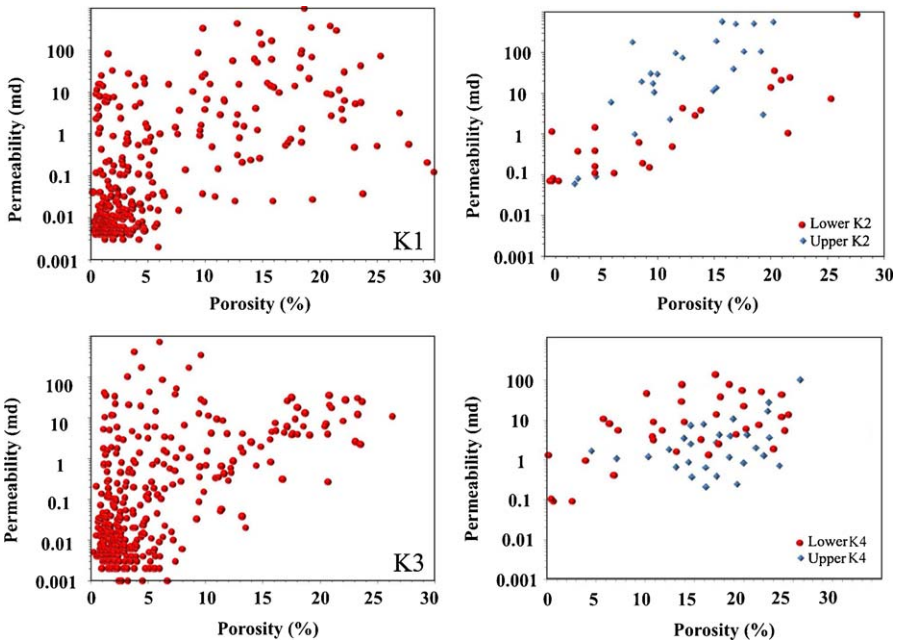

Fig. 10. Plot of permeability versus porosity data obtained from wells OFA_2 and OFA_3.

Fig. 10. Diagramme de la perméabilité en fonction de la porosité, d'après les données des puits OFA_2 et OFA_3.

constructed for better perception of relationships between RQI and diagenetic classes (Fig. 12). As it could be seen in this figure, DC4 has the highest reservoir quality with the average of 0.37. This is due to the fact that porosities in this zone are the result of dissolution that was enhanced by the subsequent dolomitisation. DC1 has the lowest reservoir quality with the average of 0.12 that reflects non-fabric selective pores (primary pores without important diagenetic imprint). In spite of this fact that Class 5 has relatively higher permeability than Classes 2 and 3, reservoir quality is not very high in this zone. This is due to low porosity values of this class.

Pore-throat size distribution has been widely used for understanding the pore geometry and resulted reservoir quality (Bliefnick and Kaldi, 1996; Cerepi et al., 2003; Mancini et al., 2004; Martin et al., 1997; Taghavi et al, 2004). In upper K2, non-fabric selective classes show moderate PTS with almost high permeability and moderate porosity. In lower parts of this unit lower diagenetic classes show creation of larger PTS caused by dissolution. The story repeats again in K4, but vice versa in upper and lower parts in comparison with K2. Decreasing PTS and porosity with minor change in permeability shows the effect of dolomitisation in lower K4 unit. It is in good agreement with DCs in reservoir zones.

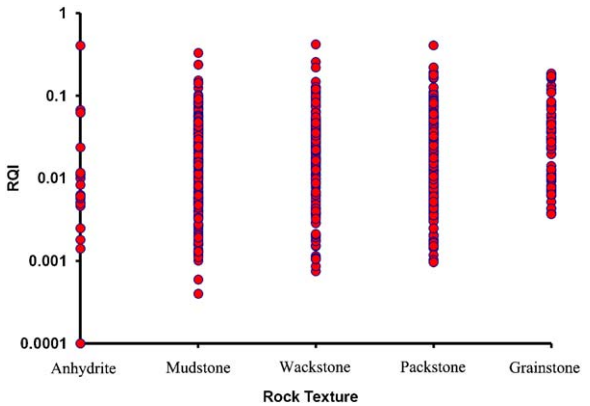

Fig. 11. Plot of rock texture versus RQI shows no obvious relationships between two parameters.

Fig. 11. Le diagramme de texture de la roche en fonction de RQI ne montre aucune relation évidente entre les deux paramètres.

Intervals with poor reservoir quality are characterized by platykurtic throat size distribution and there is obvious mode in CPC, which is shown in Fig. S3a and d. Upper K2 reservoir unit which is characterized by fabric destructive dolomitization, exhibits leptokurtic throat size distribution in Fig. S3b. Such distribution shows that pore distribution is nearly uniform and pore throats have almost the same sizes, more than 1 μm. The same trend could be seen in lower K2 unit but complementary studies (petrography and VDL log, for example) show that dissolution is the ominant connecting factor in this unit. In upper K4, where dissolution is the dominant factor for porosity and permeability creation, pore-throat size exhibit platykurtic, polymodal distribution (Fig. S3f). With increasing dolomite volume in this part, the curve tends to be flattened (Fig. S3g). Dolomites create different size connections from dissolution and so curve will be flattened. The CPC of lower K4 unit is characterizing with mesokurtic, biomodal PTS distribution. Two modes are very close to each other. Such distribution is due to fabric retentive to selective dolomitization of lower K4 unit. Same size dolomite crystals of this unit create PTS distribution shown in Fig. S3h.

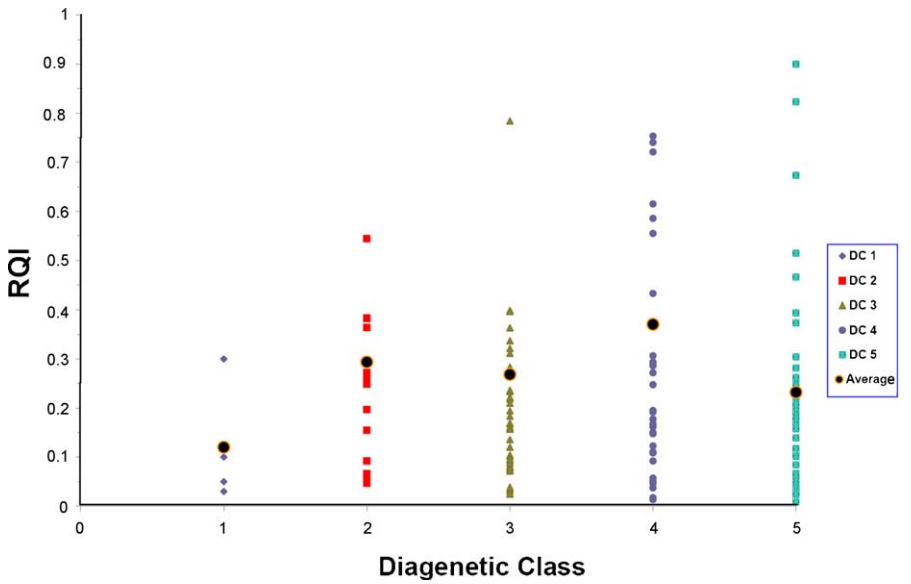

Fig. 12. Plot of diagenetic classes versus RQI show that intervals with connected fabric-selective dissolution have the best reservoir quality and non-connected primary pores have not any interest in reservoir quality point of view. Refer to text for more explanation.

Fig. 12. Le diagramme des classes diagénétiques en fonction de RQI montre que les intervalles connectés avec la dissolution sélective de texture ont la meilleure qualité de réservoir et que les pores primaires non connectés n'ont aucun intérêt du point de vue de la qualité du réservoir. Se reporter au texte pour plus d'explication.

Distribution of pore-throat sizes shows that pore system of diagenetic classes from 1 to 5 differs fundamentally from one another. This difference has a major effect on fluid-flow properties of pore systems dominated by one or the other of these systems. Moldic and fabric-selective dolomitization pore systems are heterogeneous on a microscopic scale because they consist of large pores that are connected to one another by distinctly different (commonly finer) pore systems. Note that pore sizes, but not necessarily pore-throat sizes, are inherently heterogeneous in the Class 3. By contrast, Class 5 pore system is essentially homogeneous, because they are developed in rock fabrics that tend to consist of unimodal leptokurtic distributions of dolomite crystals that are also about the same shape. It should be mentioned that there is no considerable fracturing in studied intervals in South Pars field and so permeability has no anomalously variations.

Stable isotope analysis is one of the best methods for diagenesis studies in carbonate strata (Al-Aasm and Azmy, 1996, Ehrenberg et al., 2006). Observations of stable isotope excursion trough Kangan and upper Dalan cored interval in South Pars field are indicative of $\delta^{13}C$ depletion over the PTB, concomitant with the worldwide $\delta^{13}C$ excursion at this time. The magnitude of this shift is also analogous to the other typical PTB sections in the world (e.g., Dolenec et al., 2001; Heydari and Hassanzadeh, 2003; Lehrmann et al., 2003; Korte et al., 2004; Rahimpour-Bonab et al., 2009). These findings suggest that a large input of ^{12}C-enriched carbon into the ocean-atmosphere system has occurred and may have caused a global environmental change, probably related to this greatest mass extinction in the Phanerozoic. The increasing trend toward the top (relative to PTB) has been related to restoration of primary productivity (Rahimpour-Bonab et al., 2009), while decreasing trend from bottom of the section toward the PTB could be ascribed to reoxidation of previously stored ^{12}C-enriched organic material caused by eustatic regression (Erwin, 1994; Heydari et al., 2000; Horacek et al., 2007; Loydell, 2007).

Heydari et al. (2000) related PTB isotope changes to the eustatic regression at the end Permian time. They have mentioned negative isotopic $\delta^{18}O$ values and recrystallization of lime mud matrix. In contrast, Korte et al. (2004) believe that the Late Permian sea-level fall did occur on the Russian Platform, in North America and Siberia, but a time-equivalent large-scale transgression happened in China, Iran, western Tethys and in the Zechstein Basin of central Europe. Evidences represented by thin sections and SEM studies as well as wire-line logs and stable isotopes, place more emphasis on the diagenetic origin for these isotopic anomalies. Domination of greenhouse conditions over the Early Triassic (Kidder and Worsley, 2004; Retallack, 1999) cause low (light) $\delta^{18}O$ through K2 unit.

In spite of some little differences, all three wells show similar isotope trends with well OFA_1. Comparison of stable isotopes (especially oxygen) of this well with diagenetic classes determined by detailed thin section examinations (Fig. 7) reveals some similarity. As shown in this figure, there are four distinguishable zones. Through whole of K4 and the base of the K3, diagenetic classes disperse to the fabric-selective and non-fabric selective classes (2, 3, 4 and some 5 classes). These classes are mainly fabric-selective pores which their poroperm values increased by the later fabric-destructive dolomitisation and/or dissolution. Petrographic and SEM evidences show that most of K4 unit has intercrystalline, moldic and some vuggy porosity. Regarding the nature of pore types in this interval, it could be concluded that the primary pores were

mainly enhanced by the fabric-selective dolomitisation and dissolution, but permeability improved by the non-fabric selective dolomitisation and dissolution. Decreasing trend in the $\delta^{18}O$ values accompanied with the limy lithology in the upper parts of K4 indicates domination of dissolution while the large scale dolomitisation is predominating in the lower part.

In K3 unit, with increasing $\delta^{18}O$ and $\delta^{13}C$ values, diagenetic classes shift to the higher degrees (Fig. 7, zone 2), i.e., the non-fabric selective diagenetic pores dominate. As is mentioned earlier, development of meteoric and micrite cement in K3 unit has occluded pore-throats and so reservoir quality is not high. In comparison with the planar-e dolomites of K2 and K4, poroperm values in K3 planar-s dolomites are not high. There is a high permeable zone just below the PTB that is due to grain-dominated facies. However, because of diagenetic effects these values show a dramatic decline passing the PTB interval.

After this important interval, toward K2 unit, zone 3 shows more negative $\delta^{18}O$ values. With depletion in the $\delta^{18}O$ values, diagenetic classes decrease toward the lower ones including 1, 2 and 3 (especially 1 and 3). Considering lime and dolomite lithology of K2 interval and nature of the pore types, primary porosity was enhanced by the fabric-selective dissolution and recrystallization resulted in concurrent permeability increase and reservoir quality improvement. In addition, parallel decrease in $\delta^{18}O$ values (Fig. 7), as a result of meteoric diagenesis, supports this effect.

Zone 4 is from top of the K2 to the uppermost interval (about 100 m from top of K2). This zone includes three diagenetic classes of 3, 4 and 5. There are no sharp variations in $\delta^{18}O$ and $\delta^{13}C$ values in this interval. According to diagenetic classes scheme (Fig. 6), in this zone porosity was developed mainly as intercrystalline, fracture and stylolite. Thus, observed pores are not primary and fabric-selective. Porosity volume is not high in this zone. In addition to this fact, petrographical and SEM observations showed that there is considerable volume of anhydrite in this interval that occluded most pores. This resulted in the reservoir quality loss.

Understanding the relationship between pore type and porosity and permeability in a general view is a major challenge in the evaluation of carbonate reservoirs. Here, VDL in combination with foregoing parameters employed for this purpose. In VDL point of view, the lowermost studied interval (K4) is a high quality zone with 0.85 N/G (Rahimpour-Bonab et al., 2009). VDL has average of 320 m/s in this interval that shows the dominance of the connected porosities. Ranging diagenetic classes between 2 and 5 shows that both fabric and non-fabric selective dissolution and dolomitisation are the important causes for the improvement of reservoir quality. Regarding nature of the pore types of this interval and VDL log variations, it could be concluded that primary pores were mainly enhanced by the fabric-selective dolomitisation and dissolution, while permeability improved by the non-fabric selective dolomitisation and dissolution.

In spite of well-connected porosities in the K3 unit deduced from VDL and diagenetic classes, high rate of cementation occluded pore spaces and filled pore throats imparting low reservoir quality. Generally, the VDL remains positive in the K2 while the diagenetic classes are in the range of 1 to 3. This indicates the presence of primary (Class 1) and fabric-selective diagenetic (Classes 2 and 3) pores. Domination of diagenetic Class of 5 in the uppermost of K2 is confirming the role of dolomitisation in this interval. In contrast to the K4 unit, dolomitisation is more effective in the upper parts while dissolution created reservoir quality in the lower parts of K2. Although dolomitisation decreases downward, pores are still connected that is reflected in the RQI values (Fig. 8). Fabric-selective dissolution in this interval produced important moldic porosity that has moderate connectivity. There is an increasing trend in the velocity deviation from base of the K1 unit to the top of this interval (Fig. 8). Positive values in this interval support the petrographic observations that reveal pore-filling anhydrites.

Ehrenberg et al. (2006) found similar porosity and cementation in Finnmark Formation. They showed that primary intergranular and intrafossil pores have been filled by calcite cement. Dolostones contain two dominant pore types: intercrystalline pores between dolomite crystals and moldic pores representing former bioclasts. Their study revealed that reservoir compartmentalization by the formation of tight limestone barriers is largely a burial diagenetic process involving calcite cementation locally produced by chemical compaction as could be seen here in K1 and K3 units. Eichenseer et al. (1999) believe that in Pinda Group intercrystalline porosity allows connection between moldic pores and enhances reservoir quality. Intracrystalline porosity is frequent, although volumetrically of minor importance. This is the case in lower K4 unit in our study. The same diagenetic trend has been seen by Pomar and Ward (1999) in Miocene deposits of Mallorca Island in Spain. Woody et al. (1996) note that in Cambrian–Ordovician dolomites from core and outcrop throughout southeastern Missouri, permeability displays a strong logarithmic increase with increasing porosity in planar-e dolomite. Permeability in planar-s dolomite is lower than in planar-e dolomite and does not increase as rapidly with increasing porosity. High-pressure mercury capillary pressure curves and SEM data show that planar-e dolomites are comprised of uniform well-interconnected pore systems. This is the same for K3 and K4 dolomites. Dolomites of K4 are planar-e where as K3 dolomites are planar-s in shape. Similar diagenetic trend and phases with porosity development were reported by Ehrenberg (2006), Esrafili-Dizaji and Rahimpour-Bonab (2009), Heasley et al. (2000), Kopaska-Merkel (1992), and Machel (2005).

6. Conclusions

The Permo-Triassic carbonates in the South Pars gas field have complicated diagenetic history including marine, meteoric and burial diagenesis which makes it difficult to evaluate their reservoir properties. Reservoir quality in this field is controlled by the spatial heterogeneity in diagenetic cementation, dissolution, dolomitisation and resultant porosity development. Here, an integrated approach using porosity-permeability data in

terms of RQI, mercury intrusion data, stable isotopes, petrographic studies, SEM and VDL log was used for investigating the effect of diagenesis on the reservoir quality of Kangan and Dalan formations.

There are two main reservoir zones in the Permo-Triassic interval of the studied reservoir including K2 and K4. The reservoir quality of these two zones has been mentioned previously in many studies but the clear relationship between these reservoirs and their diagenetic events in various parts had not been understood yet.

K4 is the best reservoir zone in this field with 0.85 N/G. The maximum values of porosity (average of 15.61%) and RQI are encountered in this zone. Diagenetic classes ranging mainly from 3 to 4 in the upper parts of the unit beside the higher VDL values, limy lithology and depleted $\delta^{18}O$ values all confirm the role of fabric selective dissolution in the upper parts. In the lower parts of K4, pervasive dolomitisation and intercrystalline porosity that is reflected on the diagenetic classes and VDL log, along with the petrographic observations are the evidences for the creation of secondary connectivity of the pores. In addition, primary porosities were connected following diagenetic alterations.

Most of the pores in K3 are secondary in origin but pervasive cementation caused low reservoir quality that is reflected on RQI values. The nature of pores (mainly stylolite and fractures) in this interval is another cause of low reservoir quality.

K2 has high porosity, permeability and RQI values. With average of 38.81 md, this unit has the best permeability and is one of the two main reservoir zones in the South Pars field. Depletion of stable isotope values, diagenetic classes and VDL confirm that the good quality of this zone is due to primary pores enhanced by dolomitisation in the upper parts and dissolution in the lower parts. Comparison of diagenetic classes in upper part of K2 and lower part of K4 shows some little differences. While both parts are dolomitised, in upper K2 unit non-fabric selective pores are dominant and fabric destructive dolomitisation is the main cause of high reservoir quality. In comparison, lower K4 has more fabric-selective pores that have been connected by fabric retentive to selective dolomitisation.

Diagenetic cements are heterogeneously distributed throughout the reservoir and have a maximum effect on the dominant pore network in K3 and K1 unit. Pore occluding diagenetic anhydrite is consistently most abundant in these units. Diagenetic studies in terms of diagenetic classes show secondary pores in the K1 unit. In spite of this fact, moldic nature of some pores and pervasive anhydrite cementation filled pores and occluded pore-throats. As it mentioned, RQI has low values in this zone and good reservoir intervals are not present. Results of this study show that good conclusions will achieved through integration of various data and geological concepts.

Acknowledgments

The vice-president of Research and Technology of the University of Tehran provided financial support for this research, which we are grateful. We also extend our appreciation to the POGC (Pars Oil and Gas Company of Iran) for sponsoring, data preparation, and permission to publish this paper. We would like to thank Mrs. Naderi for her detailed and helpful reviews and comments.

Appendix A. Supplementary data

Supplementary data associated with this article can be found, in the online version, at doi:10.1016/j.crte.2010.10.004.

References

Aali, J., Rahimpour-Bonab, H., Kamali, M.R., 2006. Geochemistry and origin of the world's largest gas field from Persian Gulf, Iran. J. Petrol Sci. Engin. 50, 161–175.

Abid, I., Hesse, R., 2007. Illitising fluids as precursors of hydrocarbon migration along transfer and boundary faults of the Jeanne d'Arc Basin offshore Newfoundland, Canada. Mar. Pet. Geol. 24, 237–245.

Ahr, W.M., 2008. Geology of carbonate reservoirs, the identification, description and characterisation of hydrocarbon reservoirs in carbonate rocks. Wiley Publication, New Jersey, 278 p.

Al-Aasm, I.S., Azmy, K.K., 1996. Diagenesis and evolution of microporosity of Middle–Upper Devonian Kee Scarp reefs, Norman wells, Northwest territories, Canada: petrographic and chemical evidence. AAPG Bull. 80, 82–100.

Al-Aswad, A.A., 1997. Stratigraphy, sedimentary environment and depositional evolution of the Khuff Formation in south-central Saudi Arabia. J. Pet. Geol. 20, 1–20.

Al-Husseini, M.I., 2000. Origin of the Arabian Plate Structures: Amar Collision and Najd Rift. Geo. Arabia 5, 527–542.

Alsharhan, A.S., 2006. Sedimentological character and hydrocarbon parameters of the Middle Permian to Early Triassic Khuff Formation, United Arab Emirates. GeoArabia 11, 121–158.

Alsharhan, A.S., Kendall, C., 2003. Holocene coastal carbonates and evaporites of the southern Arabian Gulf and their ancient analogues. Earth-Science Rev. 61, 191–243.

Alvarez, N.O.C., Roser, B.P., 2007. Geochemistry of black shales from the Lower Cretaceous Paja Formation, Eastern Cordillera, Colombia: Source weathering, provenance, and tectonic setting. J. South Am. Earth Sci. 23, 271–289.

Amaefule, J.O., Altunbay, M., Tiab, D., Kersey, D.G., Keelan, D.K., 1993. Enhanced Reservoir Description: Using core and log data to identify Hydraulic (Flow) Units and predict permeability in uncored intervals/wells. SPE 26436. Presented at 68th Ann. Tech. Conf. and Exhibition, Houston, TX.

Anselmetti, F.S., Eberli, G.P., 1993. Controls on sonic velocity in carbonates. Pure Appl. Geophys. 141, 287–323.

Anselmetti, F.S., Eberli, G.P., 1999. The velocity-deviation log: a tool to predict pore type and permeability trends in carbonate drill holes from sonic and porosity or density logs. AAPG Bull. 83, 450–466.

Baron, M., Parnell, J., Mark, D., Carr, A., Przyjalgowski, M., Feely, M., 2008. Evolution of hydrocarbon migration style in a fractured reservoir deduced from fluid inclusion data, Clair Field, West of Shetland, UK. Mar. Pet. Geol. 25, 153–172.

Bliefnick, D.M., Kaldi, J., 1996. Pore geometry: control on reservoir properties, Walker Creek Field, Columbia and Lafayette Counties, Arkansas. AAPG Bull. 80, 1027–1044.

Bordnave, M.L., 2008. The origin of the Permo-Triassic gas accumulations in the Iranian Zagros foldbelt and contiguous offshore area: a review of the Paleozoic petroleum system. J. Pet. Geol. 31, 3–42.

Cerepi, A., Barde, J.P., Labat, N., 2003. High-resolution characterisation and integrated study of a reservoir formation: the Danian carbonate platform in the Aquitaine Basin (France). Mar. Pet. Geol. 20, 1161–1183.

Choquette, P.W., Pray, L.C., 1970. Geologic nomenclature and classification of porosity in sedimentary carbonates. AAPG Bull. 54, 207–250.

Dolenec, T., Lojen, S., Ramovs, A., 2001. The Permian-Triassic boundary in western Slovenia (Idrijca Valley section): magnetostratigraphy, stable isotopes, and elemental variations. Chem. Geol. 175, 175–190.

Ehrenberg, S.N., 2006. Porosity destruction in carbonate platforms. J. Pet. Geol. 29, 41–52.
Ehrenberg, S.N., Aqrawi, A.A.M., Nadeau, P.H., 2008. An overview of reservoir quality in producing Cretaceous strata of the Middle East. Pet. Geosci. 14, 307–318.
Eichenseer, H.T., Walgenwitz, F.R., Biondi, P.J., 1999. Stratigraphic control on facies and diagenesis of dolomitized oolitic siliciclastic ramp sequences (Pinda Group, Albian, offshore Angola). AAPG Bull. 83, 1729–1758.
Elias, A.R., Ros, D.L.F., Mizusaki, A.M., Anjos, S.M., 2004. Diagenetic patterns in eolian/coastal sabkha reservoirs of the Solimoes Basin, northern Brazil. Sed. Geol. 169, 191–217.
Erwin, D.H., 1994. The Permo-Triassic extinction. Nature 367, 231–236.
Esrafili-Dizaji, B., Rahimpour-Bonab, H., 2009. Effects of depositional and diagenetic characteristics on carbonate reservoir quality: a case study from the South Pars gas field in the Persian Gulf. Pet. Geosci. 15, 1–22.
Gardner, G.H.F., Gardner, L.W., Gregory, A.R., 1974. Formation velocity and density: the diagnostic basics for stratigraphic traps. Geophysics 39, 770–780.
Guadagno, F.M., Nunziata, C., 1993. Seismic velocities of fractured carbonate rocks (southern Apennines, Italy). Geophys. J. Int. 113, 739–746.
Halley, R.B., Harris, P.M., 1979. Freshwater cementation of a 1000-year-old-oolite. J. Sed. Pet. 49, 969–988.
Heasley, E.C., Worden, R.H., Hendry, J.P., 2000. Cement distribution in a carbonate reservoir: recognition of a palaeo oil-water contact and its relationship to reservoir quality in the Humbly Grove Field, onshore, UK. Mar. Pet. Geol. 17, 639–654.
Heydari, E., Hassanzadeh, J., 2003. Deev Jahi model of the Permian-Triassic mass extinction: a case study for gas hydrates as the main cause of biological crisis on earth. J. Sed. Geol. 163, 147–163.
Heydari, E., Hassanzadeh, J., Wade, W.J., 2000. Geochemistry of central tethyan Upper Permian and Lower Triassic strata, Abadeh region, Iran. J. Sed. Geol. 137, 85–89.
Hilchie, D.W., 1982. Advanced well log interpretation. Golden, Colorado, 300 p.
Horacek, M., Brandner, R., Abart, R., 2007. Carbon isotope record of the P/T boundary and the Lower Triassic in the Southern Alps: evidence for rapid changes in storage of organic carbon. Paleogeogr. Palaeoclimatol. Palaeoecol. 252, 347–354.
Insalaco, E., Virgone, A., Courme, B., Gaillot, J., Kamali, M., Moallemi, A., Lotfpour, M., Monibi, S., 2006. Upper Dalan Member and Kangan Formation between the Zagros Mountains and offshore Fars, Iran: depositional system, biostratigraphy and stratigraphic architecture. GeoArabia 11, 75–176.
James, N.P., Choquette, P.W., 1984. Diagenesis of Limestones; the meteoric diagenetic environment. Geosci. Can. 11, 161–194.
Kashfi, M.S., 2000. Greater Persian Gulf Permian–Triassic stratigraphic nomenclature requires study. Oil and Gas Journal 6, 36–44.
Kidder, D.L., Worsley, T.R., 2004. Causes and consequences of extreme Permo-Triassic warming to globally equable climate and relation to the Permo-Triassic extinction and recovery. Paleogeogr. Palaeoclimatol. Palaeoecol. 203, 207–237.
Kirmaci, M.Z., 2008. Dolomitisation of the Late Cretaceous–Palaeocene platform carbonates, Gölköy (Ordu), eastern Pontides, NE Turkey. Sedimentary Geology 203, 289–306.
Konert, G., Afif, A.M., AL-Hajari, S.A., Droste, H., 2001. Palaeozoic stratigraphy and hydrocarbon habitat of the Arabian Plate. GeoArabia 6, 407–442.
Kopaska-Merkel, D.C., 1992. Geologic setting, petrophysical characteristics, and regional heterogeneity patterns of the Smackover in Southwest Alabama. In: Geological Survey of Alabama, .
Kopaska-Merkel, D.C., Mann, S.D., 1994. Classification of lithified carbonates using ternary plots of pore facies-examples from the Jurassic Smackover Formation, Carbonate microfabrics symposium proceedings, Texas A and M University, College Station, Texas. In: Frontiers in Sedimentary Geology Series, p. 265–277.
Korte, C., Kozur, H.W., Joachimski, M.M., Strauss, H., Veizer, J., Schwark, L., 2004. Carbon, sulfur, oxygen and strontium isotope records, organochemistry and biostratigraphy across the Permian/Triassic boundary in Abadeh, Iran. Geol. Rundsch 93, 565–581.
Lehrmann, D.J., Payne, J.L., Flix, S.V., Dilllet, P.M., 2003. Permian-Triassic boundary sections form shallow marine carbonate platforms of the Nanpanjiang basin, south China: implications for oceanic conditions associated with the end Permian extinction and its aftermath. Palaios 18, 138–152.
Loydell, D.K., 2007. Early Silurian positive $\delta^{13}C$ excursions and their relationship to glaciations, sea-level changes and extinction events. Geol. J. 42, 531–546.
Lucia, F.J., 1999. Carbonate reservoir characterization. Springer, 226 p.
Lucia, F.J., 2007. Carbonate reservoir characterisation: an integrated approach, 2nd. edition. Springer, 336 p.
Machel, H.G., 2005. Investigations of burial diagenesis in carbonate hydrocarbon reservoir rocks. Geosci. Can. 32, 103–128.
Mancini, E.A., Llinas, J.C., Parcell, W.C., Aurell, M., Badenas, B., Leinfelder, R.R., Benson, D.J., 2004. Upper Jurassic thrombolite reservoir play, northeastern Gulf of Mexico. AAPG Bull. 88, 1573–1602.
Martin, A.J., Solomon, S.T., Hartmann, D.J., 1997. Characterization of petrophysical flow units in carbonate reservoirs. AAPG Bull. 81, 734–759.
Moore, C.H., 2001. Carbonate reservoirs: porosity evolution and diagenesis in a sequence stratigraphic framework. Amsterdam, Elsevier, 460 p.
Moradpour, M., Zamani, Z., Moallemi, S.A., 2008. Controls on reservoir quality in the Lower Triassic Kangan Formation, Southern Persian Gulf. J. Petrol. Geol. 31, 367–386.
Nur, A., Simmons, G., 1969. The effect of saturation on velocity in low porosity rocks. Earth Planet. Sci. Lett. 7, 183–193.
Pomar, L., Ward, W.C., 1999. Reservoir-scale heterogeneity in depositional packages and diagenetic patterns on a reef-rimmed platform, Upper Miocene, Mallorca, Spain. AAPG Bull. 83, 1759–1773.
Rahimpour-Bonab, H., 2007. A procedure for appraisal of a hydrocarbon reservoir continuity and quantification of its heterogeneity. J. Petrol. Sci. Engin. 58, 1–12.
Rahimpour-Bonab, H., Asadi-Eskandar, A., Sonei, A., 2009. Controls of Permian-Triassic Boundary over Reservoir Characteristics of South Pars Gas Field, Persian Gulf. Geol. J. 44, 341–364.
Rahimpour-Bonab, H., Esrafili-Dizaji, B., Tavakoli, V., 2010. Dolomitization and anhydrite precipitation in Permo-Triassic carbonates at the South Pars gas Field, Offshore Iran: controls on reservoir quality. J. Pet. Geol. 33, 43–66.
Retallack, G.J., 1999. Postapocalyptic greenhouse paleoclimate revealed by Earliest Triassic paleosols in the Sydney Basin, Australia. Geol. Soc. Am. Bull. 111, 52–70.
Schlumberger, 1974. Log interpretation-applications, Vol. 2. Schlumberger Limited, 116 p.
Stentoft, N., Lapinskas, P., Musteikis, P., 2003. Diagenesis of Silurian reefal carbonates, Kudirka oilfield, Lithuania. J. Petrol. Geol. 26, 381–402.
Szabo, F., Keradpir, A., 1978. Permian and Triassic stratigraphy Zagros Basin, Southwest Iran. J. Petrol. Geol. 1, 57–82.
Taghavi, A.A., Mork, A., Emadi, M.A., 2006. Sequence stratigraphically controlled diagenesis governs reservoir quality in the carbonate Dehluran Field, Southwest Iran. Petrol. Geosci. 12, 115–126.
Tucker, M.E., Bathurst, R.G.C., 1990. Carbonate Diagenesis. Blackwell Scientific Publications, Oxford, 320 p.
Videtich, P.E., 1994. Dolomitization and H2S generation in the Permian Khuff Formation, Offshore Dubai, UAE. Carbonates and Evaporites 9, 42–57.
Woody, R.E., Gregg, J.M., Koederitz, L.F., 1996. Dolomite: evidence from the Cambrian-Ordovician of southeastern Missouri. AAPG Bull. 80, 119–132.
Wyllie, G., Gardner, G.H.F., 1956. Elastic wave velocities in heterogeneous and porous media. Geophysics 21, 41–70.